

## Article

# C2-Hydrocarbon Mixture Separation on Polyethylene Membranes with Grafted Sulfonated Polystyrene in H<sup>+</sup>, Li<sup>+</sup> and Na<sup>+</sup> Forms

Natalya Zhilyaeva <sup>1</sup>, Evgeny Sofronov <sup>1</sup>, Elena Mironova <sup>1</sup>, Nina Shevlyakova <sup>2</sup>, Vladimir Tverskoy <sup>2</sup>, Irina Stenina <sup>3</sup>  and Andrey Yaroslavtsev <sup>1,3,\*</sup> 

- <sup>1</sup> A.V. Topchiev Institute of Petrochemical Synthesis, Russian Academy of Sciences, Leninsky Prospekt 29, Moscow 119991, Russia; zhilyaeva@ips.ac.ru (N.Z.); zhenya.sofronov.00@mail.ru (E.S.); palukas@ips.ac.ru (E.M.)
- <sup>2</sup> Lomonosov Institute of Fine Chemical Technologies, MIREA—Russian Technological University, Moscow 119454, Russia; shevlyakova@mitht.ru (N.S.); vladimirtverskoj@gmail.com (V.T.)
- <sup>3</sup> Kurnakov Institute of General and Inorganic Chemistry, Russian Academy of Sciences, Leninsky Prospekt 31, Moscow 119991, Russia; stenina@igic.ras.ru
- \* Correspondence: yaroslav@igic.ras.ru; Tel.: +7-(495)-7756585

**Abstract:** The olefin separation from their mixture with paraffins by facilitated transport membranes is a very important process for the further macromolecular compounds production. Membranes loaded with silver ions, which are responsible for the facilitated olefin transport, are instable with time due to their reduction, while those containing protons catalyze the polymerization of olefins. In this work, membranes based on polyethylene with grafted sulfonated polystyrene in various ionic forms (H<sup>+</sup>, Li<sup>+</sup>, Na<sup>+</sup>) were used for the first time for the separation of the ethylene/ethane mixture. The influence of sulfonation time, relative humidity, and various ionic forms on ethylene separation was studied. The SEM study shows a non-uniform sulfur distribution over the membrane thickness for membranes sulfonated for different reaction times. With increasing sulfonation time and relative humidity the ethylene permeability and the factor of its separation with ethane increase. Separation factors for membranes in the Li<sup>+</sup>-form are shown to be as high as for membranes in the H<sup>+</sup>-form. A possible mechanism for the facilitated ethylene transport is discussed.

**Keywords:** C2-hydrocarbon separation; sulfonated polystyrene; ion exchange membrane; facilitated ethylene transport; ethylene; olefin



**Citation:** Zhilyaeva, N.; Sofronov, E.; Mironova, E.; Shevlyakova, N.; Tverskoy, V.; Stenina, I.; Yaroslavtsev, A. C2-Hydrocarbon Mixture Separation on Polyethylene Membranes with Grafted Sulfonated Polystyrene in H<sup>+</sup>, Li<sup>+</sup> and Na<sup>+</sup> Forms. *Processes* **2023**, *11*, 2489. <https://doi.org/10.3390/pr11082489>

Academic Editor: Fausto Gallucci

Received: 23 July 2023

Revised: 11 August 2023

Accepted: 17 August 2023

Published: 18 August 2023



**Copyright:** © 2023 by the authors. Licensee MDPI, Basel, Switzerland. This article is an open access article distributed under the terms and conditions of the Creative Commons Attribution (CC BY) license (<https://creativecommons.org/licenses/by/4.0/>).

## 1. Introduction

Olefins are among the most important reagents in the chemical and petroleum industries. The main method for their production is the pyrolysis of ethane, propane, naphtha, or gas oil. This technology is energy consuming. Since it results in the production of olefin/paraffin mixtures, it should include an olefin separation processes such as distillation, adsorption, and extraction [1,2]. The complexity of the olefin/paraffin separation is due to their similar molecular weights, sizes, and volatility. Moreover, current separation methods, e.g., cryogenic distillation, are very energy-intensive [3].

Energy-saving and environmentally friendly membrane technologies are more preferable for the olefin/paraffin separation [4–7]. At present, polymer membranes are successfully used in a number of gas separation processes, such as the carbon dioxide separation from a mixture with nitrogen [8–11] and hydrogen purification [12,13]. However, selectivity of membranes used in such processes is insufficient for an efficient olefin separation from saturated hydrocarbons. When using a gas mixture, phenomena of competitive sorption, plasticization, and others affect the transport of the gas mixture components and can lead to a decrease in separation selectivity [14].

Facilitated transport in membrane processes attracts the attention of researchers due to efficient separation performance [15–20]. It is well known that some transition metal cations, for example,  $\text{Ag}^+$  and  $\text{Cu}^+$ , form  $\pi$ -complexes with olefins, which leads to an increase in selectivity [21]. It has recently been shown that the facilitated transport mechanism is also realized in ion-exchange polymeric membranes in the  $\text{H}^+$ -form [22], which are widely used in a number of technological processes [23–30]. A number of works showed a significant effect of ion-exchange capacity on the transport properties of ion-exchange membranes [31–34], e.g., in composite cation-exchange membranes based on main-chained sulfonated polyethersulfone and polyvinylpyrrolidone, both the hydrophilicity and the ionic conductivity increase with an increase in the sulfonation degree [32]. An increase in the sulfonation degree leads to a higher density of ion clusters and an increase in the pore size, resulting in ion transport acceleration in sulfocationite membranes. It was shown that a decrease in the ethylene content in a mixture with paraffins led to an increase in its separation factor (the selectivity) [35]. It is known that the transport of ions in ion-exchange membranes occurs through a system of pores and channels filled with water molecules. Therefore, the rate of such transfer significantly depends on the membrane water uptake. Complexes of cations containing olefins should be transported in the same way. The effect of humidity on the selectivity of separation by sulfonic acid ion-exchange membranes was shown in the works [35–37]. Since the ethylene transport occurs via a  $\pi$ -complex, which can be formed not only with d-elements but also with protons differing only by a high positive charge density [35], the question arises about possibilities of using ion-exchange membranes containing alkali metal cations with small ionic radius ( $\text{Li}^+$ ,  $\text{Na}^+$ ), which are not prone to participate in redox reactions and the olefin polymerization, for the olefin/paraffin separation. It should be noted that, to the best of our knowledge, there are currently no such studies in the literature.

In this work, we studied for the first time the influence of various ionic forms ( $\text{Li}^+$ ,  $\text{Na}^+$ ) of membranes based on polyethylene with radiation-grafted sulfonated polystyrene on the selectivity of ethylene/ethane transport. The effect of the sulfonation time of polystyrene and the humidity of the gas flow was also studied.

## 2. Materials and Methods

### 2.1. Membrane Preparation

Styrene (analytical standard grade) was obtained from Sigma-Aldrich (St. Louis, MO, USA). Iron(II) sulfate heptahydrate (chemical purity grade), methanol (reagent grade), HCl (reagent grade), and NaOH (reagent grade) were obtained from Chimmed (Moscow, Russia).

The low-density polyethylene-g-polystyrene sulfonic acid membranes (S-LDPE-g-PS) were prepared using post-radiation grafting polymerization of styrene on a low-density polyethylene (PE) film of 12  $\mu\text{m}$  thickness, followed by polystyrene (PS) sulfonation with sulfuric acid (96 wt. %) according to the procedure described in previous paper [22]. Irradiation of polyolefins in air is accompanied by their radiation-chemical oxidation. The graft polymerization can be initiated by peroxide radicals and hydroperoxides, the concentration of which depends on both the peroxide concentration and the concentration of iron (II) salts, which act as inhibitors of styrene homopolymerization in the graft solution and peroxide reducers. In our case, to form peroxides, PE films were irradiated in air using a  $^{60}\text{Co}$   $\gamma$ -radiation source at a dose rate of 5.2 Gy/s for a predetermined time.

The post-radiation chemical graft polymerization was carried out using a mixture of styrene/methanol at a ratio of 1:1 by volume with iron (II) sulfate. Styrene was washed with a 30% aqueous solution of NaOH to remove the inhibitor, then with distilled water to remove the excess of alkali until a neutral reaction of washwater was reached, and dried over calcined calcium chloride. After that, styrene was distilled under vacuum and a fraction of 46  $^{\circ}\text{C}$  was taken at a residual pressure of 11 mm Hg. The degree of grafting (the proportion of the grafted polystyrene,  $\Delta p$ ) was calculated as the ratio of the weight

gain of the membrane after grafting to the weight of PE film before grafting. The degree of grafting for the membranes was 110%.

Sulfuric acid (96 wt. %) was used as the sulphurizing agent. The sulfonation of low-density polyethylene-g-polystyrene films was carried out at a temperature of 98 °C. After that, films were washed with a diluted aqueous solution of sulfuric acid and distilled water until a neutral reaction of washwater was reached. A preliminary IR spectroscopy study showed that fully sulfonated PE-g-polystyrene could be prepared at a sulfonation time of 3 h [22]. In this regard, to study the effect of the sulfonation degree on transport and gas separation properties of membranes, the latter were sulfonated for 20, 60, 120, and 210 min. The effect of the counterion ( $H^+$ ,  $Li^+$ , and  $Na^+$ ) nature on the ethylene/ethane transport was studied for the membranes in  $H^+$ -,  $Li^+$ -, and  $Na^+$ -form prepared by keeping them in 0.1 M solutions of the corresponding hydroxides for 2 h, followed by washing with deionized water until a neutral reaction of washwater.

## 2.2. Membrane Characterization

To determine the ion-exchange capacity (IEC), weighed membranes dried at 80 °C were kept in 0.1 M NaOH solution for 24 h. After that, the test from the solution was titrated with 0.1 M HCl solution. The IEC was calculated using Equation (1):

$$IEC = \{V_{NaOH} \cdot N_{NaOH} - V_{HCl} (V_{NaOH}/V) \cdot N_{HCl}\} / m, \quad (1)$$

where  $V_{NaOH}$  is the NaOH solution volume in which the membrane was kept;  $V_{HCl}$  is the HCl solution volume used for NaOH solution titration;  $V$  is the NaOH solution volume using for the titration with HCl solution;  $N_{NaOH}$  and  $N_{HCl}$  are NaOH and HCl solution titres, respectively; and  $m$  is the membrane weight.

IR spectra were recorded on a Nicolet iS5 (Thermo Fisher Scientific, Madison, WI, USA) with a Quest Specac diamond crystal, recording parameters: spectral range 4000–550  $cm^{-1}$ , resolution 2  $cm^{-1}$ , 50 scans.

The membrane morphology and sulfur distribution over the membrane thickness were studied using a Tescan Amber scanning electron microscope (Tescan, Czech Republic) equipped with an Oxford Instruments elemental microanalysis attachment.

## 2.3. Gas Permeability Study

A scheme of the setup for the gas permeability study is shown in Figure 1. To study the gas separation properties of the prepared membranes, the ethylene/ethane mixture in a ratio of 9:91 (*vol.:vol.%*) came from mixer 1, passed through pressure gauge 2, and entered bubbler 4 with distilled water kept at a certain temperature by a thermostat. This is due to the fact that the gases entering the membrane cell must be moistened, since the permeability of the studied polymer membranes depends on the degree of their hydration. The ratio of hydrocarbons was chosen based on previous studies [22].

The humidification was carried out simultaneously on both sides of a membrane to avoid a moisture gradient across the membrane. Therefore, helium also passed through bubbler 3 under the same conditions. Relative humidity (RH, %) was determined at the outlet of the membrane cell with an AR847 temperature and humidity meter (“Smart Sensor”, Dongguan, China). The relative humidity of the initial gas mixture was changed from 30 to 80% by changing the temperature of the bubbler with distilled water. The time of the gas pre-saturation was 2 h.

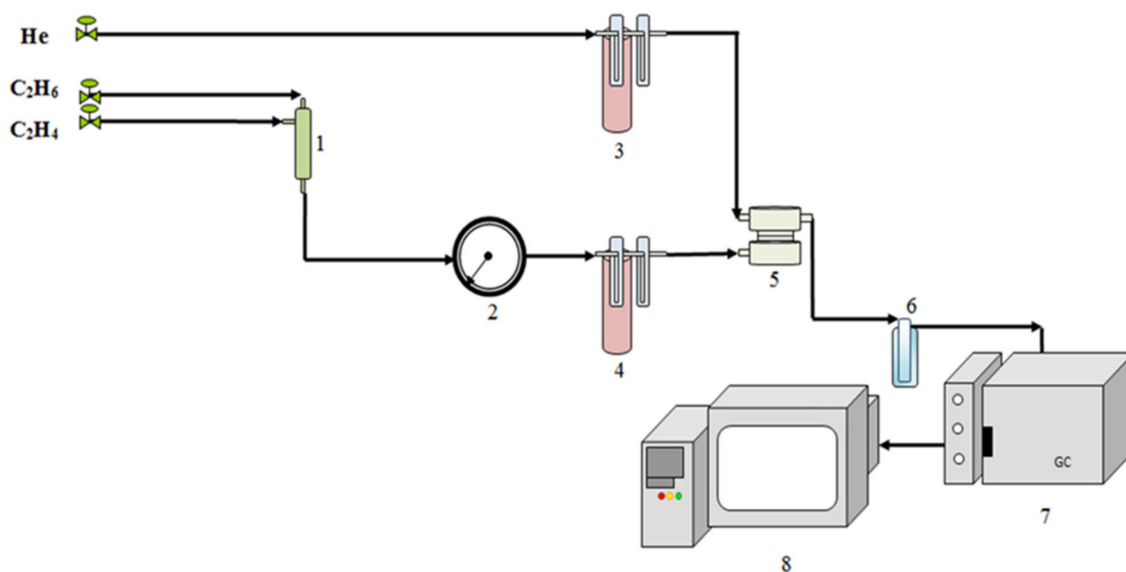


**Figure 1.** Scheme of the setup for the gas permeability study: 1—mixer; 2—manometer; 3, 4—bubblers; 5—membrane cell; 6—trap; 7—gas chromatograph; 8—computer.

Ethylene/ethane permeability was studied in a stainless steel cell (Figure 1) divided by a membrane into two non-communicating compartments. The membrane area was  $3.46 \text{ cm}^2$ . A  $\text{C}_2\text{H}_4:\text{C}_2\text{H}_6$  gas mixture was supplied to one compartment (retentate); a carrier gas (helium) was passed through another compartment (permeate).

#### 2.4. Analysis of Separation Products

Gas concentrations in both chambers were determined using a Kristallux 4000M gas chromatograph (“Meta-chrom”, Yoshkar-Ola, Russia) with a Porapak Q-“Supelco” column (Bellefonte, Pennsylvania, USA) and a thermal conductivity detector. The permeability coefficient  $P$  ( $\text{cm}/(\text{cm}^2 \text{ s atm})$ ) was calculated using Equation (2):

$$P = V_{\text{sg}} \cdot d \cdot C_i / \{S \cdot (p_1 - p_2)(C_i^0 - C_i)\}, \quad (2)$$

where  $V_{\text{sg}}$  is the sweep gas rate;  $d$  and  $S$  are the membrane thickness and area, respectively;  $C_i$  is the gas concentration in the permeate;  $p_1$  is the partial pressure in the retentate;  $p_2$  is the partial pressure in the permeate; and  $C_i^0$  is the gas concentration in the initial gas mixture (retentate). The value of  $P$  is expressed in Barrer ( $1 \text{ Barrer} = 10^{-10} \text{ cm}^3 (\text{nc}) \text{ cm}/(\text{cm}^2 \text{ s cm Hg})$ ). The gas separation factor was determined as the ratio of the gas permeability coefficients.

### 3. Results and Discussion

IR spectroscopy data confirm a successful sulfonation of the LDPE-g-PS membranes (Figure 2). IR spectra of the prepared membranes show a combination of bands of the original PE matrix and the grafted sulfonated polystyrene. The most intense pair of bands in the range of  $2920\text{--}2850 \text{ cm}^{-1}$  was ascribed to the asymmetric and symmetric stretching vibrations of the  $-\text{CH}_2-$  groups of polyethylene and aliphatic C-H groups of polystyrene (Figure 2). In the range of  $1380\text{--}1500 \text{ cm}^{-1}$ , there are bands of bending vibrations of polyethylene groups and C-C stretching vibrations of polystyrene (Figure 2). The band at  $695 \text{ cm}^{-1}$  was attributed to out-of-plane bending vibrations of polystyrene (the aromatic  $-\text{CH}$  bond).

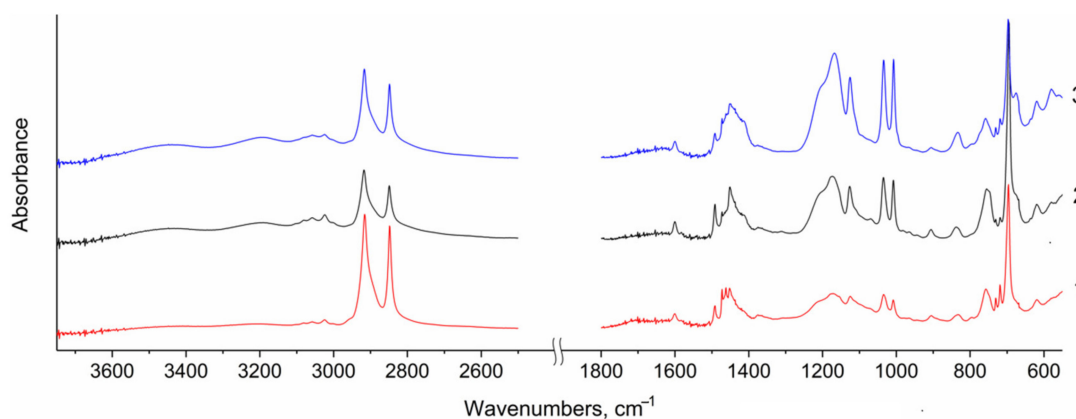


**Figure 2.** IR spectra of the prepared S-LDPE-g-PS membranes sulfonated for: 1—20 min; 2—1 h; 3—3.5 h.

A number of new bands appeared after membrane sulfonation. A weakly resolved doublet with maxima at  $1170$  and  $1200\text{ cm}^{-1}$  and a separate band at  $1125\text{ cm}^{-1}$ , related to antisymmetric and symmetric stretching vibrations, and also the band at  $670\text{ cm}^{-1}$  of bending vibrations show the presence of sulfonic acid groups ( $-\text{SO}_3\text{H}$ ). The intensity of these bands increases as the time of sulfonation of the studied membranes increases (Figure 2). The appearance of an intense band at  $835\text{ cm}^{-1}$  ascribed to out-of-plane bending vibrations of C–H bonds in the benzene ring indicates the addition of sulfonyl group predominantly at the para position. It should be noted that the analysis of changes in the intensity of bands of the unsubstituted phenyl and sulfonic acid groups allows the authors of work [22] to confirm the conclusion that the process of sulfonation with sulfuric acid is a diffusion-limited process. At the same time, after sulfonation for 3.5 h, practically no unsubstituted phenyl groups remained.

The sulfonation of the prepared materials is accompanied by their significant hydration due to the absorption of water from the atmosphere. Therefore, broad bands with maxima at  $3450$  and  $3200\text{ cm}^{-1}$  appear in the range of O–H stretching vibrations (Figure 2). At the same time, the intensity of poorly resolved bands with maxima in the range  $1640$ – $1710\text{ cm}^{-1}$ , ascribed to the deformation vibrations of water and  $\text{H}_3\text{O}^+$  or  $\text{H}_5\text{O}_2^+$  ions, increases. The intensity of the first of them increases relative to the second with increasing sulfonation time. This somewhat unexpected phenomenon occurs because the formation of new hydrophilic clusters in the membrane facilitates the absorption of additional water due to the formation of hydrogen bonds of the  $\text{H}_2\text{O}$ –H–OH type.

The ion-exchange capacity of the prepared membranes increases with increasing sulfonation time (Table 1).

**Table 1.** Ion exchange capacity for membranes sulfonated for different reaction times.

Sulfonation Time	IEC, mg Eq/g	Sulfonation Degree, %
20 min	1.9	44
1 h	2.6	65
2 h	2.9	75
3.5 h	3.6	100

The gas permeability and separation factor significantly depend on the sulfonation degree of the membranes obtained. For a non-sulfonated film of the LDPE-g-PS copolymer, the ethylene and ethane permeabilities are similar and vary slightly with humidity change. For membranes in the  $\text{H}^+$ -form prepared for a minimal sulfonation time (20 min), the permeabilities of both ethane and ethylene at RH = 50% increase slightly, while the separation factor remains almost unchanged (Figures 3 and 4). With increasing humidity, the ethylene permeability for this sample changes slightly (Figure 1), while the ethane

permeability decreases markedly. As a result, the separation factor is slightly increased (Figure 4). More significant changes occur for membranes with increased sulfonation time. The ethylene permeability increases significantly, especially at high humidity, while the ethane permeability, on the contrary, decreases (Figure 3). As a result, the ethylene/ethane separation factor reaches 4.2 at RH = 80% for the membrane sulfonated for 3.5 h (Figure 4).

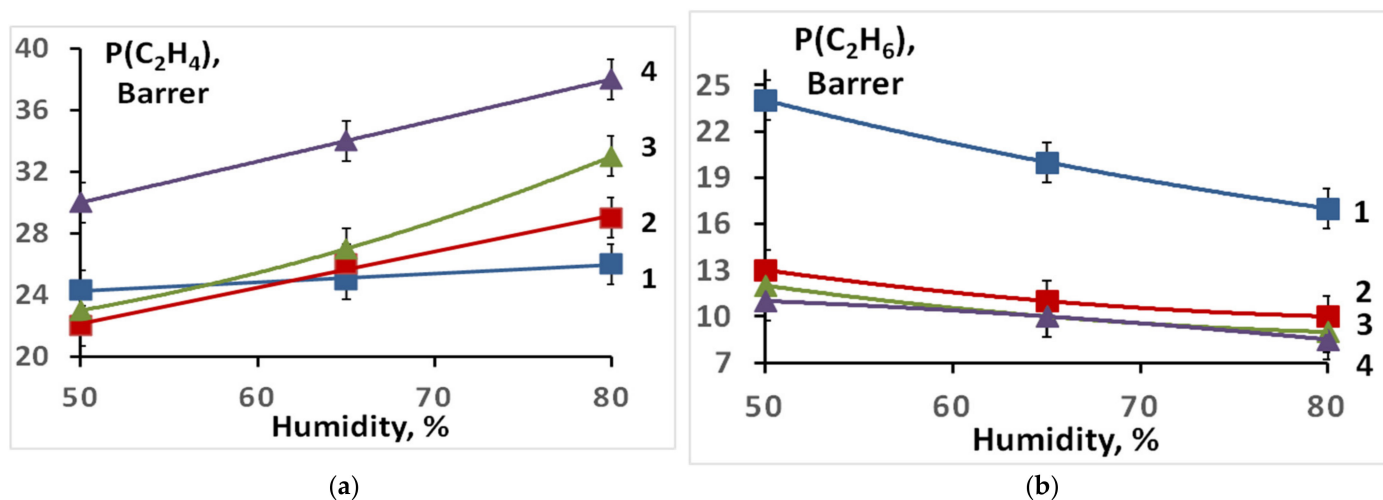


**Figure 3.** Ethylene (a) and ethane (b) permeability coefficients for the prepared S-PE-g-PS membranes (in the  $H^+$ -form) sulfonated for: 1—20 min; 2—1 h; 3—2 h; 4—3.5 h.

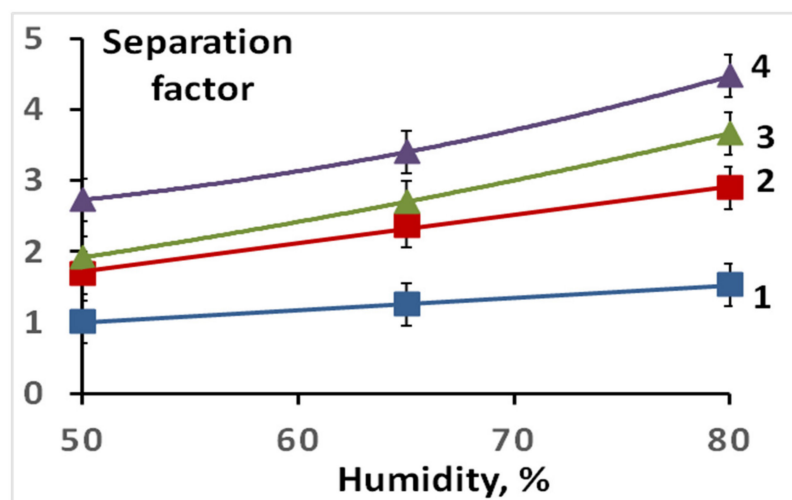


**Figure 4.** Separation factors for the prepared S-PE-g-PS membranes (in the  $H^+$ -form) sulfonated for: 1—20 min; 2—1 h; 3—2 h; 4—3.5 h.

To understand the results obtained, let us consider the data of scanning electron microscopy and energy-dispersive X-ray microanalysis of membranes sulfonated for different times (Figure 5). All membranes are continuous polymer films. The prepared membranes belong to the type of homogeneous ion-exchange membranes [38]. Hydrophilic regions of PFSA membranes are presented by pores connected by channels [39,40]. The average pore size is 3–5 nm and depends strongly on the membrane's water uptake [34,41]. A model describing their structure was proposed by Gierke et al. on the basis of small-angle X-ray scattering data for Nafion membranes [42]. It should also be mentioned that there is a strong correlation between water uptake, transport properties of ion-exchange membranes, and relative humidity [43,44].

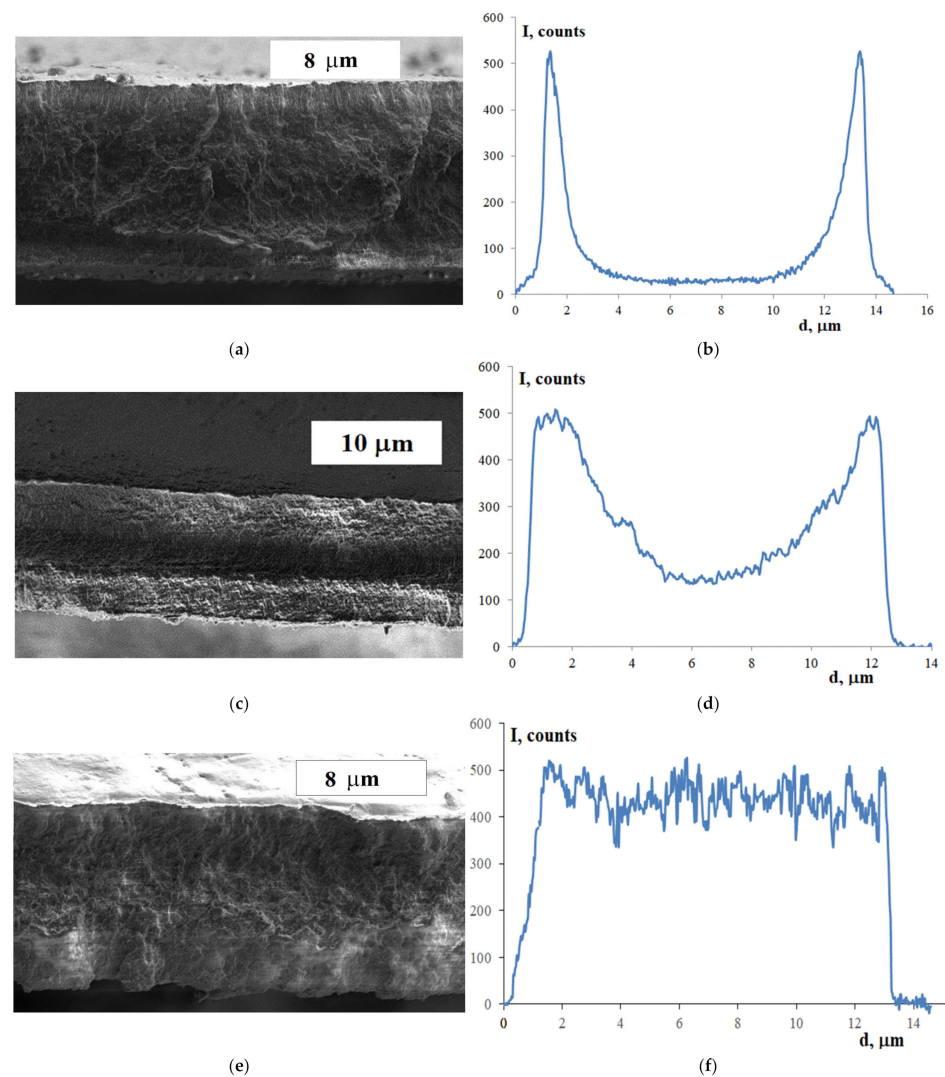


**Figure 5.** SEM images (a,c,e) and sulfur distribution (b,d,f) over membrane thickness for the membranes sulfonated for: (a,b)—20 min, (c,d)—1 h, (e,f)—3.5 h.

Pores in such membranes cannot be detected even using transmission electron microscopy, since they disappear when the chamber with samples is evacuated (high resolution electron microscopy requires samples to be imaged under high vacuum). Their presence was described only after special studies using small-angle X-ray scattering [42]. Therefore, our goal was, first of all, to analyze the distribution of sulfur over the membrane thickness, which gave fairly clear and unambiguous results. If the bulk of the LDPE-g-PS film sulfonated for 20 min seems to be homogeneous and somewhat different from the surface, the surface layers of the LDPE-g-PS film sulfonated for 1 h differ significantly from the central part (Figure 5a). As the sulfonation time increases, the films become homogeneous again (Figure 5c).

This tendency is even more clearly manifested in Figure 5b,d,f, which shows the sulfur distribution over the membrane thickness obtained using EDX spectroscopy and SEM. Both membranes sulfonated for 20 and 60 min have surfaces enriched with sulfonic acid groups (Figure 5b,d). At the same time, membranes prepared using sulfonation for 20 min have an inner layer in which there are almost no sulfonic acid groups (Figure 5b). The sulfonic acid group concentration in the central part of the membrane with the sulfonation time of 1 h is about 35% relative to the membrane surface (Figure 5d). Finally, with an increase in the sulfonation time up to 3.5 h, the distribution of sulfonic acid groups over the membrane thickness becomes almost uniform (Figure 5f), which is consistent with the fact

that the sulfonation degree reaches 100% for this sample. This is due to the autocatalytic nature of the sulfonation process noted in [45]. The membrane sulfonation leads to the formation of polar material in which the sulfuric acid solubility is much higher, and the sulfonation occurs much faster than would be expected from Fick's law. The reason for this is an increase in the acid diffusion rate in sulfonated layers of polystyrene.

According to the data obtained, the degree of sulfonation of membranes significantly increases with an increase in the time of contact of the LDPE-g-PS film with the sulfonating agent (sulfuric acid). At the same time, the central part of membranes sulfonated for 20 min contains few sulfonic acid groups, and its morphology is almost identical to the morphology of the pristine LDPE-g-PS film. For membranes sulfonated for 1 h, about 35% of the central part is sulfonated (Figure 5c). Based on the diffusion and autocatalytic nature of kinetics of sulfonation reactions, it can be assumed that, in this case, separate channels with a sufficiently high degree of sulfonation are formed in the central part of the S-LDPE-g-PS membrane. Finally, after 3.5 h, the sulfonation is completed and the membrane becomes homogeneous again.

Based on the data obtained, it can be concluded that for membranes with a sulfonation time of 20 min, the gas diffusion is determined by their permeability through the non-sulfonated inner polymer layers. This is also confirmed by the fact that the ethylene permeability for this sample remains practically constant within the error. Since the sizes of ethane and ethylene molecules are similar, their transport rates are also close, and the separation factor remains close to unity. As the sulfonation time increases, the ethylene permeability increases, while the ethane permeability, on the contrary, decreases. With further sulfonation, the ethylene permeability increases, and the selectivity, initially changed slightly, increases significantly for membranes sulfonated for 3.5 h. In this case, both the ethylene permeability and the selectivity increase noticeably with increasing the gas mixture humidity.

This is determined by the fact that for membranes with high sulfonation degrees, the ethylene transport occurs both through the hydrophobic part of a membrane, which does not contain sulfonic acid groups, and through membrane pores containing sulfonic acid groups and water. Moreover, in the latter, facilitated transport of ethylene is realized in the form of its complex with protons. These complexes form due to the interaction of proton with a double C=C bond of ethylene, which has an increased electron density. In this case,  $C_2H_3^+$  cations are formed, the cross section of which, perpendicular to the direction of the double bond, is comparable to the size of potassium or rubidium ions. As a result, like these cations, it is hydrated and easily moves in an aqueous solution localized in the system of pores and channels of the S-LDPE-g-PS ion-exchange membrane. Similarly, the transfer of the proton–ethylene complex is significantly accelerated with an increase in the degree of membrane hydration (water uptake), i.e., with an increase in the gas mixture humidity. At the same time, it should be noted that ethylene moves in the hydrophobic matrix as neutral molecules, while in hydrophilic regions it moves as the charged complex. Its transition from one state to another is associated with the protonation/deprotonation of the complex and proceeds relatively slowly. That is why the rate of ethylene transfer increases with increasing humidity, the faster, the higher the degree of its sulfonation due to the formation of a more developed system of pores and channels. A well-bound system of hydrophilic pores, through which a charged complex is continuously transported, is formed only in membranes sulfonated for 3.5 h, and therefore the ethylene transport reaches a maximum rate.

On the contrary, non-polar ethane molecules, which are not capable of forming complexes with protons, hardly dissolve in hydrophilic membrane pores filled with water, and are effectively displaced from them due to a sufficiently high field strength of the electric double layer formed by negatively charged pore walls and positively charged protons in the membrane pores. Therefore, it can be assumed that ethane transfer proceeds only through the hydrophobic polymer matrix. As the relative humidity increases, the proportion of the hydrophobic matrix in the membrane decreases, which leads to a slowdown in the ethane



transfer. Together with a significant increase in the ethylene transfer rate, this leads to a sharp increase in selectivity with an increase in the degree of membrane sulfonation and relative humidity.

Relatively small lithium and sodium cations, as well as protons, can form complexes with ethylene interacting with the increased electron density of its C=C double bond. However, the larger the cation size and its polarizing ability, the lower the strength of these complexes. Therefore, the membrane conversion from the H<sup>+</sup>- to the Li<sup>+</sup>- and the Na<sup>+</sup>-form leads to a decrease in ethylene permeability. The highest permeabilities of membranes in the Li<sup>+</sup>- and Na<sup>+</sup>-forms are 12.8 and 1.5 Barrer, respectively (Figure 6), while the permeability of the same membrane in the H<sup>+</sup>- form reaches 28 Barrer. Such a decrease in the permeability upon the membrane conversion from the H<sup>+</sup>- to the Li<sup>+</sup>- and the Na<sup>+</sup>-form is due to a gradual decrease in the strength of the ethylene complex with the corresponding cation in the series H<sup>+</sup> > Li<sup>+</sup> > Na<sup>+</sup> (Figure 6). In this case, the separation factors for the H<sup>+</sup>- and Li<sup>+</sup>-forms are similar and higher than those for the Na<sup>+</sup>-form (Figure 7). The selectivity, as expected, increases with the humidity of the gas mixture and membrane water uptake. Moreover, it should be noted that separation factors of membranes loaded with lithium and sodium ions do not change for 100 h.

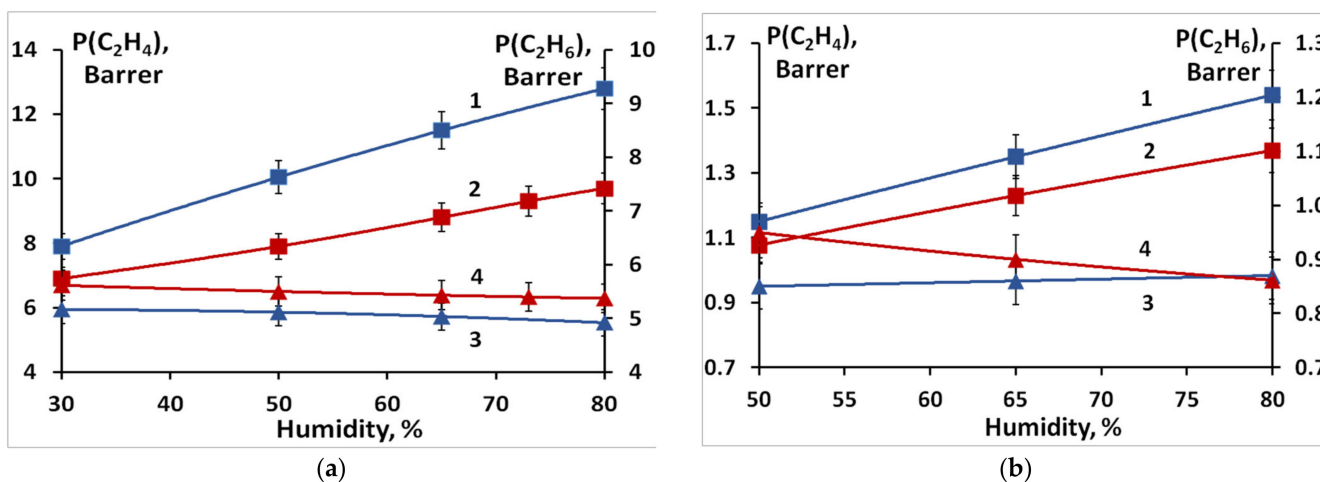


**Figure 6.** Ethylene (1, 2) and ethane (3, 4) permeability coefficients at different relative humidity for the prepared S-PE-g-PS membranes in the Li<sup>+</sup>- (a) and Na<sup>+</sup>-form (b) sulfonated for: 1, 3—1 h; 2, 4—2 h.

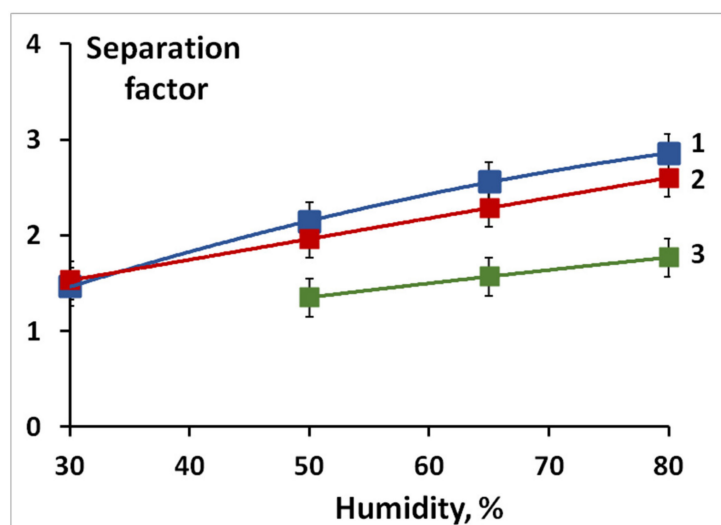


**Figure 7.** Separation factors at different relative humidity for various ionic forms of membranes sulfonated for 1 h: 1—H<sup>+</sup>; 2—Li<sup>+</sup>; 3—Na<sup>+</sup>.

It is worth discussing the significance of the results obtained. The S-LDPE-g-PS membranes prepared in this work are not optimal for the separation of ethane/ethylene mixtures and are inferior to the composite membranes based on nanoporous films coated with a thin Nafion layer in Ag<sup>+</sup>-form reported in ref. [36] in terms of transfer rate and separation selectivity. At the same time, the separation factors for these membranes in the H<sup>+</sup>-form are close to those obtained in this work. However, both methods for separating mixtures of olefins and paraffins using membranes in silver and hydrogen forms have certain disadvantages. For example, silver ions in the membrane matrix are quickly reduced not only under light, but also due to interaction with ethylene, which leads to the loss of their activity in separation processes [35,46]. Membranes in the H<sup>+</sup>-form are more stable; however, they, as strong acids, induce ethylene polymerization, which leads to a decrease in ethylene permeability through the prepared S-LDPE-g-PS membranes by 23% within 50 h. At the same time, the S-LDPE-g-PS membranes in the Li<sup>+</sup>-form retained their permeability and selectivity within the same time.

#### 4. Conclusions

In this work, the separation of an ethylene/ethane mixture with the use of membranes based on polyethylene with grafted sulfonated polystyrene with different sulfonation times was studied. It has been shown that with an increase in the sulfonation time, the ethylene permeability and separation selectivity increase. The SEM method was used to study the distribution of sulfur over the membrane thickness. It should be noted that this work shows for the first time the possibility of achieving high separation factors for membranes in the lithium form, which are close to those for the hydrogen form. This is important, since the lithium form, unlike the silver one is stable (it cannot be easily reduced) and does not catalyze the polymerization of olefins, leading to their loss and a gradual membrane degradation, as the hydrogen form does. For the sodium, Na<sup>+</sup>-form, the separation effect is less pronounced. A possible mechanism for the facilitated ethylene transport on the membranes prepared is discussed.

**Author Contributions:** Conceptualization, V.T. and A.Y.; methodology, V.T. and A.Y.; validation, E.S., N.S. and A.Y.; investigation, N.Z., E.M., E.S., N.S. and I.S.; resources, N.Z., N.S. and V.T.; data curation, E.M., E.S., N.S. and A.Y.; writing—original draft preparation, N.Z., N.S. and V.T.; writing—review and editing, N.Z., I.S. and A.Y.; visualization, N.Z., E.M., I.S. and A.Y.; supervision, V.T. and A.Y. All authors have read and agreed to the published version of the manuscript.

**Funding:** This research received no external funding.

**Data Availability Statement:** The data presented in this study are available upon request from the corresponding author.

**Acknowledgments:** This work was carried out within the framework of the State Assignment of the A.V. Topchiev Institute of Petrochemical Synthesis, Russian Academy of Sciences. This research was performed using the equipment of the JRC PMR IGIC RAS.

**Conflicts of Interest:** The authors declare no conflict of interest.

#### References

1. Sholl, D.S.; Lively, R.P. Seven chemical separations to change the world. *Nature* **2016**, *532*, 435–437. [[CrossRef](#)] [[PubMed](#)]
2. Yi, S.; Ghanem, B.; Liu, Y.; Pinnau, I.; Koros, W.J. Ultrasensitive glassy polymer membranes with unprecedented performance for energy-efficient sour gas separation. *Sci. Adv.* **2019**, *5*, 5459. [[CrossRef](#)] [[PubMed](#)]
3. Xu, M.; Jiang, B.; Dou, H.; Yang, N.; Xiao, X.; Tantai, X.; Sun, Y.; Zhang, L. Customized facilitated transport membranes by mixed strategy for ethylene/ethane separation. *Sep. Purif. Technol.* **2021**, *277*, 119484. [[CrossRef](#)]
4. Valadez Sanchez, E.P.; Gliemann, H.; Haas-Santo, K.; Ding, W.; Hansjosten, E.; Wohlgemuth, J.; Woll, C.; Dittmeyer, R.  $\alpha$ -Al<sub>2</sub>O<sub>3</sub>-supported ZIF-8 SURMOF membranes: Diffusion mechanism of ethene/ethane mixtures and gas separation performance. *J. Membr. Sci.* **2020**, *594*, 117421. [[CrossRef](#)]
5. Malakhov, A.O.; Bazhenov, S.D.; Vasilevsky, V.P.; Borisov, I.L.; Ovcharova, A.A.; Bilyukevich, A.V.; Volkov, V.V.; Giorno, L.; Volkov, A.V. Thin-film composite hollow fiber membranes for ethylene/ethane separation in gas-liquid membrane contactor. *Sep. Purif. Technol.* **2019**, *219*, 64–73. [[CrossRef](#)]

6. Jiang, B.; Zhou, J.; Xu, M.; Dou, H.; Zhang, H.; Yang, N.; Zhang, L. Multifunctional ternary deep eutectic solvent-based membranes for the cost-effective ethylene/ethane separation. *J. Membr. Sci.* **2020**, *610*, 118243. [[CrossRef](#)]
7. Wang, C.; Yan, J.; Ma, Z.; Wang, Z. Highly efficient separation of ethylene/ethane in microenvironment-modulated microporous polymers. *Sep. Purif. Technol.* **2022**, *287*, 120580. [[CrossRef](#)]
8. Sekizkardes, A.K.; Budhathoki, S.; Zhu, L.; Kusuma, V.; Tong, Z.; McNally, J.S.; Steckel, J.A.; Yi, S.; Hopkinson, D. Molecular design and fabrication of PIM-1/polyphosphazene blend membranes with high performance for CO<sub>2</sub>/N<sub>2</sub> separation. *J. Membr. Sci.* **2021**, *640*, 119764. [[CrossRef](#)]
9. Kojabad, M.E.; Babaluo, A.; Tavakoli, A. A novel semi-mobile carrier facilitated transport membrane containing aniline/poly(ether-block-amide) for CO<sub>2</sub>/N<sub>2</sub> separation: Molecular simulation and experimental study. *Sep. Purif. Technol.* **2021**, *266*, 118494. [[CrossRef](#)]
10. Zheng, W.; Tian, Z.; Wang, Z.; Peng, D.; Zhang, Y.; Wang, J.; Zhang, Y. Dual-function biomimetic carrier based facilitated transport mixed matrix membranes with high stability for efficient CO<sub>2</sub>/N<sub>2</sub> separation. *Sep. Purif. Technol.* **2022**, *285*, 120371. [[CrossRef](#)]
11. Alent'ev, A.Y.; Volkov, A.V.; Vorotyntsev, I.V.; Maksimov, A.L.; Yaroslavtsev, A.B. Membrane technologies for decarbonization. *Membr. Membr. Technol.* **2021**, *3*, 255–273. [[CrossRef](#)]
12. Han, Y.; Ho, W.S.W. Facilitated transport membranes for H<sub>2</sub> purification from coal-derived syngas: A techno-economic analysis. *J. Membr. Sci.* **2021**, *636*, 119549. [[CrossRef](#)]
13. Basov, N.L.; Ermilova, M.M.; Orekhova, N.V.; Yaroslavtsev, A.B. Membrane catalysis in the dehydrogenation and hydrogen production processes. *Russ. Chem. Rev.* **2013**, *82*, 352–368. [[CrossRef](#)]
14. Checchetto, R. Accurate monitoring of gas mixture transport kinetics through polymeric membranes. *Sep. Purif. Technol.* **2021**, *277*, 119477. [[CrossRef](#)]
15. Merkel, T.C.; Blanc, R.; Ciobanu, I.; Firat, B.; Suwarlim, A.; Zeid, J. Silver salt facilitated transport membranes for olefin/paraffin separations: Carrier instability and a novel regeneration method. *J. Membr. Sci.* **2013**, *447*, 177–189. [[CrossRef](#)]
16. Yu, G.; Zhang, L.; Alhumaydhi, I.A.; Abdeltawab, A.A.; Bagabas, A.A.; Al-Megren, H.A.; Al-Deyab, S.S.; Chen, X. Separation of propylene and propane by alkyimidazolium thiocyanate ionic liquids with Cu<sup>+</sup> salt. *Sep. Purif. Technol.* **2015**, *156*, 356–362. [[CrossRef](#)]
17. Dou, H.; Jiang, B.; Zhang, L.; Xu, M.; Sun, Y. Synergy of high permeability, selectivity and good stability properties of silver-decorated deep eutectic solvent based facilitated transport membranes for efficient ethylene/ethane separation. *J. Membr. Sci.* **2018**, *567*, 39–48. [[CrossRef](#)]
18. Wang, D.; Liu, F.; Zhang, X.; Wu, M.; Wang, F.; Liu, J.; Wang, J.; Liu, Q.; Zeng, H. A Janus facilitated transport membrane with asymmetric surface wettability and dense/porous structure: Enabling high stability and separation efficiency. *J. Membr. Sci.* **2021**, *626*, 119183. [[CrossRef](#)]
19. Hong, C.-H.; Ahmad, N.N.R.; Leo, C.P.; Ahmad, A.L.; Mohammad, A.W. Progress in polyvinyl alcohol membranes with facilitated transport properties for carbon capture. *J. Environ. Chem. Eng.* **2021**, *9*, 106783. [[CrossRef](#)]
20. Min, J.G.; Kemp, K.C.; Hong, S.B. Silver ZK-5 zeolites for selective ethylene/ethane separation. *Sep. Purif. Technol.* **2020**, *250*, 117146. [[CrossRef](#)]
21. Davenport, M.N.; Bentley, C.L.; Brennecke, J.F.; Freeman, B.D. Ethylene and ethane transport properties of hydrogen-stable Ag<sup>+</sup>-based facilitated transport membranes. *J. Membr. Sci.* **2022**, *647*, 120300. [[CrossRef](#)]
22. Zhilyaeva, N.A.; Mironova, E.Y.; Ermilova, M.M.; Orekhova, N.V.; Bondarenko, G.N.; Dyakova, M.G.; Shevlyakova, N.V.; Tverskoy, V.A.; Yaroslavtsev, A.B. Polyethylene-graft-sulfonated polystyrene membranes for the separation of ethylene–ethane mixtures. *Petr. Chem.* **2016**, *56*, 1034–1041. [[CrossRef](#)]
23. Hosseini, S.M.; Jashni, E.; Habibi, M.; Nemati, M.; Van der Bruggen, B. Evaluating the ion transport characteristics of novel graphene oxide nanoplates entrapped mixed matrix cation exchange membranes in water deionization. *J. Membr. Sci.* **2017**, *541*, 641–652. [[CrossRef](#)]
24. Radmanesh, F.; Rijnaarts, T.; Moheb, A.; Sadeghi, M.; de Vos, W.M. Enhanced selectivity and performance of heterogeneous cation exchange membranes through addition of sulfonated and protonated Montmorillonite. *J. Colloid Interface Sci.* **2019**, *533*, 658–670. [[CrossRef](#)]
25. Sharma, P.P.; Yadav, V.; Rajput, A.; Gupta, H.; Saravaia, H.; Kulshrestha, V. Sulfonated poly(ether ether ketone) composite cation exchange membrane for selective recovery of lithium by electrodialysis. *Desalin. Water Treat.* **2020**, *496*, 114755. [[CrossRef](#)]
26. Shukla, G.; Shahi, V.K. Sulfonated poly(ether ether ketone)/imidized graphene oxide composite cation exchange membrane with improved conductivity and stability for electrodialytic water desalination. *Desalin. Water Treat.* **2019**, *451*, 200–208. [[CrossRef](#)]
27. Klose, C.; Breitwieser, M.; Vierrath, S.; Klingele, M.; Cho, H.; Büchler, A.; Kerres, J.; Thiele, S. Electrospun sulfonated poly(ether ketone) nanofibers as proton conductive reinforcement for durable Nafion composite membranes. *J. Power Sources* **2017**, *361*, 237e242. [[CrossRef](#)]
28. Goel, P.; Mandal, P.; Bhuvanesh, E.; Shahi, V.K.; Chattopadhyay, S. Sulfonated poly(ether ether ketone) composite cation exchange membrane for NaOH production by electro-electrodialysis using agro-based paper mill green liquor. *J. Environ. Chem. Eng.* **2021**, *9*, 106409. [[CrossRef](#)]
29. Avci, A.H.; Rijnaarts, T.; Fontananova, E.; Di Profio, G.; Vankelecom, I.F.V.; De Vos, W.M.; Curcio, E. Sulfonated polyethersulfone based cation exchange membranes for reverse electrodialysis under high salinity gradients. *J. Membr. Sci.* **2020**, *595*, 117585. [[CrossRef](#)]

30. Titorova, V.D.; Moroz, I.A.; Mareev, S.A.; Pismenskaya, N.D.; Sabbatovskii, K.G.; Wang, Y.; Xu, T.; Nikonenko, V.V. How bulk and surface properties of sulfonated cation-exchange membranes response to their exposure to electric current during electro dialysis of a  $\text{Ca}^{2+}$  containing solution. *J. Membr. Sci.* **2022**, *644*, 120149. [[CrossRef](#)]
31. Stránská, E. Relationships between transport and physical–mechanical properties of ion exchange membranes. *Desalin. Water Treat.* **2015**, *56*, 3220–3227. [[CrossRef](#)]
32. Zhao, J.; Guo, L.; Wang, J. Synthesis of cation exchange membranes based on sulfonated polyether sulfone with different sulfonation degrees. *J. Membr. Sci.* **2018**, *563*, 957–968. [[CrossRef](#)]
33. Prikhno, I.A.; Safronova, E.Y.; Stenina, I.A.; Yurova, P.A.; Yaroslavtsev, A.B. Dependence of the transport properties of perfluorinated sulfonated cation-exchange membranes on ion-exchange capacity. *Membr. Membr. Technol.* **2020**, *2*, 265–271. [[CrossRef](#)]
34. Mareev, S.; Gorobchenko, A.; Ivanov, D.; Anokhin, D.; Nikonenko, V. Ion and water transport in ion-exchange membranes for power generations: Guidelines for modeling. *Int. J. Mol. Sci.* **2023**, *24*, 34. [[CrossRef](#)]
35. Zhilyaeva, N.; Mironova, E.; Ermilova, M.; Orekhova, N.; Dyakova, M.; Shevlyakova, N.; Tverskoi, V.; Yaroslavtsev, A. Facilitated transport of ethylene through the polyethylene-graft-sulfonated polystyrene membranes. The role of humidity. *Sep. Purif. Technol.* **2018**, *195*, 170–173. [[CrossRef](#)]
36. Volkov, A.O.; Golubenko, D.V.; Yaroslavtsev, A.B. Development of solid polymer composite membranes based on sulfonated fluorocopolymer for olefin/paraffin separation with high permeability and selectivity. *Sep. Purif. Technol.* **2021**, *254*, 117562. [[CrossRef](#)]
37. Zhilyaeva, N.A.; Lytkina, A.A.; Mironova, E.Y.; Ermilova, M.M.; Orekhova, N.V.; Shevlyakova, N.V.; Tverskoy, V.A.; Yaroslavtsev, A.B. Polyethylene with radiation-grafted sulfonated polystyrene membranes for butane and butenes separation. *Chem. Eng. Res. Des.* **2020**, *161*, 253–259. [[CrossRef](#)]
38. Jiang, S.; Sun, H.; Wang, H.; Ladewig, B.P.; Yao, Z. A comprehensive review on the synthesis and applications of ion exchange membranes. *Chemosphere* **2021**, *282*, 130817. [[CrossRef](#)]
39. Kusoglu, A.; Weber, A.Z. New insights into perfluorinated sulfonic-acid ionomers. *Chem. Rev.* **2017**, *117*, 987–1104. [[CrossRef](#)]
40. Yaroslavtsev, A.B.; Stenina, I.A.; Golubenko, D.V. Membrane materials for energy production and storage. *Pure Appl. Chem.* **2020**, *92*, 1147–1157. [[CrossRef](#)]
41. Xiong, P.; Zhang, L.; Chen, Y.; Peng, S.; Yu, G. A Chemistry and Microstructure Perspective on Ion-Conducting Membranes for Redox Flow Batteries. *Angew. Chem. Int. Ed.* **2021**, *60*, 24770–24798. [[CrossRef](#)]
42. Hsu, W.Y.; Gierke, T.D. Ion transport and clustering in nafion perfluorinated membranes. *J. Membr. Sci.* **1983**, *13*, 307–326. [[CrossRef](#)]
43. Choi, S.Y.; Ikhsan, M.M.; Jin, K.S.; Henkensmeier, D. Nanostructure-Property Relationship of Two Perfluorinated Sulfonic Acid (PFSA) Membranes. *Int. J. Energy Res.* **2022**, *46*, 11265–11277. [[CrossRef](#)]
44. Nikonenko, V.; Pismenskaya, N. Ion and Molecule Transport in Membrane Systems 3.0 and 4.0. *Int. J. Mol. Sci.* **2023**, *24*, 8211. [[CrossRef](#)]
45. Golubenko, D.V.; Malakhova, V.R.; Yurova, P.A.; Evsiunina, M.V.; Stenina, I.A. Effect of Sulfonation Conditions on Properties of Ion-Conducting Membranes Based on Polystyrene Grafted on Gamma-Irradiated Polyvinylidene Fluoride Films. *Membr. Membr. Technol.* **2022**, *4*, 267–275. [[CrossRef](#)]
46. Kang, S.W.; Kim, J.H.; Char, K.; Won, J.; Kang, Y.S. Nanocomposite silver polymer electrolytes as facilitated olefin transport membranes. *J. Membr. Sci.* **2006**, *285*, 102–107. [[CrossRef](#)]

**Disclaimer/Publisher’s Note:** The statements, opinions and data contained in all publications are solely those of the individual author(s) and contributor(s) and not of MDPI and/or the editor(s). MDPI and/or the editor(s) disclaim responsibility for any injury to people or property resulting from any ideas, methods, instructions or products referred to in the content.